Short communication

High-power LiFePO$_4$ cathode materials with a continuous nano carbon network for lithium-ion batteries

Jin-Ming Chen [a], Chia-Haw Hsu [a], Yu-Run Lin [a], Mei-Hui Hsiao [a], George Ting-Kuo Fey [b],*

[a] Material Chemical Laboratories, Industrial Technology Research Institute, Hsinchu 310, Taiwan
[b] Department of Chemical and Materials Engineering, National Central University, Chung-Li 320, Taiwan

ARTICLE INFO

ABSTRACT

To meet the requirements of high-power products (ex. electric scooters, hybrid electric vehicles, pure electric vehicles and robots), high-energy safe lithium-ion batteries need to be developed in the future. This research will focus on the microstructures and electrochemical properties of olivine-type LiFePO$_4$ cathode materials. The morphologies of LiFePO$_4$/C composite materials show spherical-type particles and have good carbon conductive networks. From the TEM bright field image and EELS mapping, the LiFePO$_4$/C powder shows continuous, dispersive nano-carbon network. These structures will improve electron transfer and lithium-ion diffusion for LiFePO$_4$ cathode materials, and increase their conductivity from 10^{-9} S cm^{-1} to 10^{-3} S cm^{-1}. The electrochemical properties of LiFePO$_4$/C cathode material in this work demonstrated high rate capability ($\geq$12 C) and long cycle life ($\geq$700 cycles at a 3 C discharge rate).

1. Introduction

Since the pioneering work of Goodenough and co-workers in 1997 [1], olivine LiFePO$_4$ cathode materials are being commercialized because of their low toxicity, low cost, long cycle life and cell safety which make them particularly attractive for high-power applications such as robots, power tools, electric scooters, hybrid electric vehicles, and pure electric vehicles. The theoretical specific capacity of LiFePO$_4$ is 170 mAh g^{-1}, but its poor rate capability which has been attributed to low electronic conductivity prevents its use in high-power applications. Improvements in rate capability have been achieved and reported in many research papers [2–6], including mixing in fine particles [7], particle-size control [8], doping with a conducting metal ion [9] and carbon coating [10]. Many kinds of carbon coating methods are used to increase the electronic conductivity of LiFePO$_4$. These methods contain the post synthesis [11] by cogrinding and cofiring with organic or polymetric additives [12,13] to produce coated particles. Larger amounts of carbon will increase rate capability and reduce volumetric energy density of the cathode. However, the amount and structure of carbon content will strongly influence the electronic conductivity of LiFePO$_4$/C composite materials. Therefore, to avoid decreasing the volumetric

energy density, the amount of carbon should be kept low and more efficient. The LiFePO$_4$/C composite materials which have a continuous and dispersive nano-carbon network show high electronic conductivity and rate capability. A newly carbon-coated structure of LiFePO$_4$/C composite materials that has a nano-carbon network was investigated in this work.

2. Experimental

2.1. Synthesis procedure

LiFePO$_4$ was synthesized from a stoichiometric mixture of reagent grade NH$_4$H$_2$PO$_4$ (Alfa-Aesar), CH$_3$COOLi (Aldrich), and FeC$_2$O$_4$·2H$_2$O (Aldrich) by a conventional solid-state reaction method. These materials were ground for 20 min, then pressed into pellets and heated at 623 K in a quartz-tube furnace with flowing nitrogen gas for 6 h. After slowly cooling to room temperature, pellets were ground again for 20 min and up to 6 wt.% copolymer (guluronic acid) was added to the samples. The guluronic acid powder was ground and dissolved in the alcohol solution. These samples were heated to 973 K at a heating rate of approximately 3 K min^{-1} and held at that temperature for 10 h in order to derive the LiFePO$_4$/C composite materials. After solid-state reaction, the total carbon content of LiFePO$_4$/C powder was measured by EA. These carbons were obtained from the synthesized precursors and guluronic acid.

* Corresponding author. Tel.: +886 3 425 7325; fax: +886 3 425 7325.
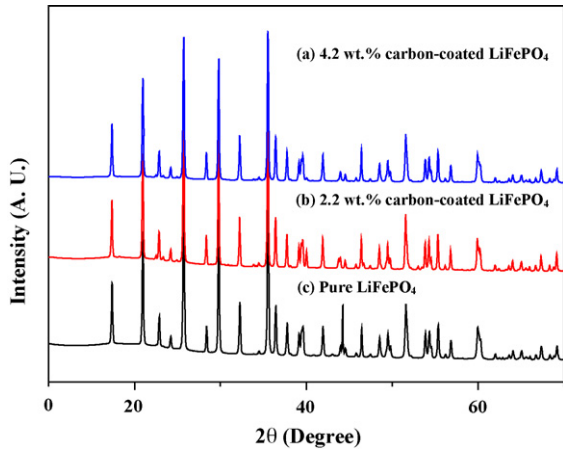E-mail address: gfey@cc.ncu.edu.tw (G.T.-K. Fey).

Fig. 1. Typical synchrotron X-ray diffraction patterns of LiFePO$_4$ (pure) and LiFePO$_4$/C powders.

2.2. Structural and morphological characterization

All samples were analyzed for phase and purity by X-ray diffraction (XRD) on the samples using a Philips PW1700 diffractometer with Cu Kα radiation ($\lambda = 1.54$ Å). Particle-size distributions were resolved by means of a Beckman counter particle-size analyzer (model LS230). The particle morphology studies were conducted using a field-emission scanning electron microscope (FE-SEM, JEOL JSM-6340F). The transmission electron microscope bright field image and EELS mapping are used to find the microstructure and nano-carbon channels of pure LiFePO$_4$ and LiFePO$_4$/C powder. The transmission electron microscope bright field image and EELS mapping were observed by using a transmission electron microscope (TEM, JEOL JEM-2010) equipped with an energy-dispersive X-ray spectrometer (EDS). To find the iron disorder and impurities that were caused by the reduction of iron during the carbon coating process, synchrotron radiation experiments were used. The synchrotron X-ray diffraction experiments were also conducted at the SRC (Synchrotron Radiation Center, Taiwan). The sample, mounted
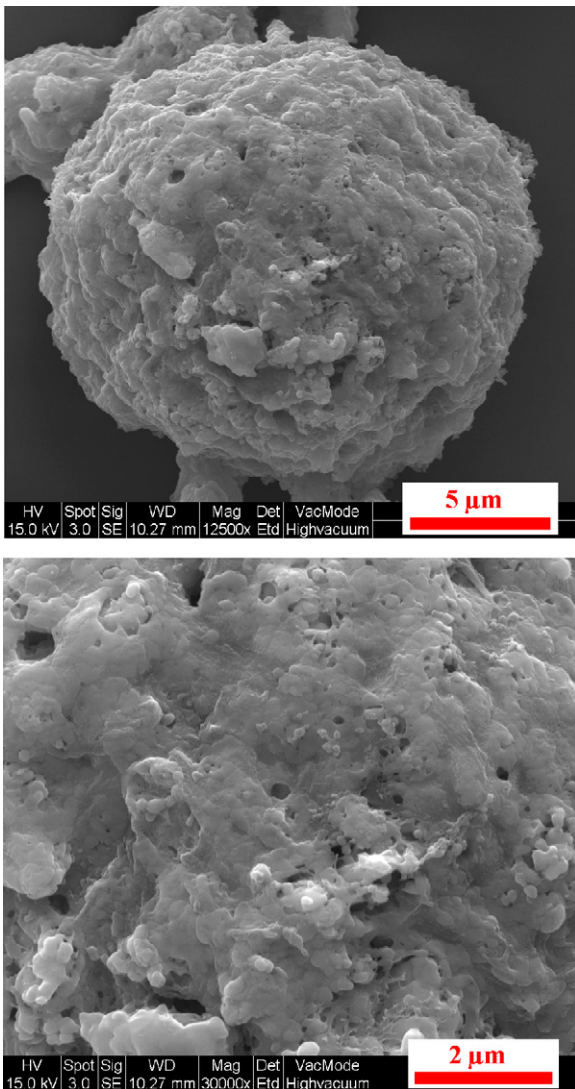

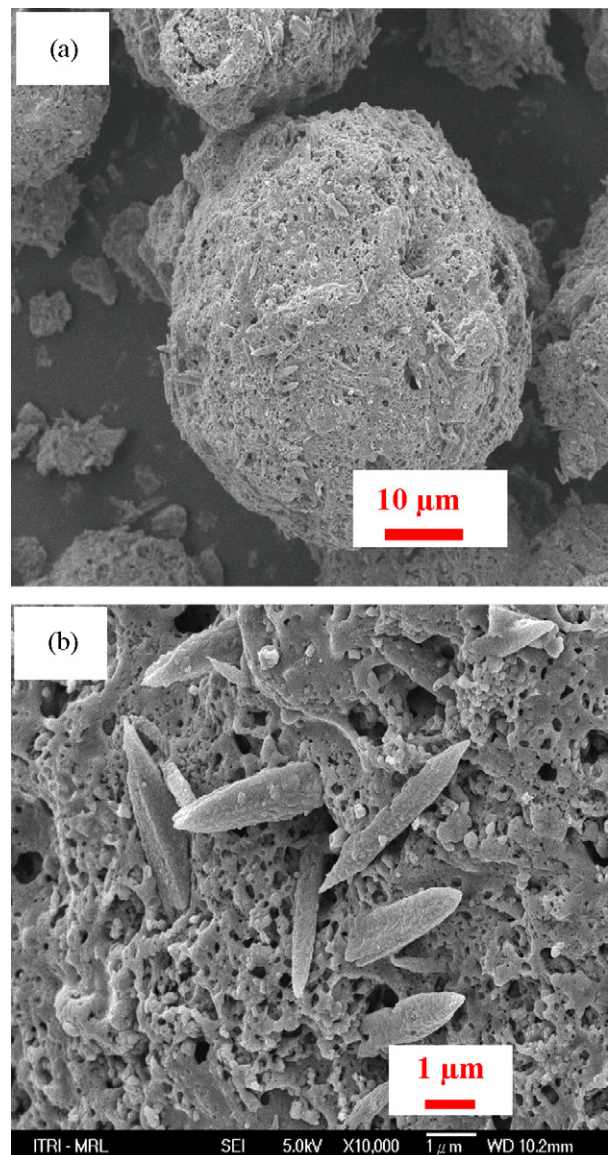**Fig. 2.** The surface morphology of LiFePO$_4$ (pure) powders.

Fig. 3. The surface morphology of LiFePO$_4$/C powders.

Sample	LiFePO$_4$ (pure)	LiFePO$_4$/C
BET surface area (m^2 g^{-1})	8	22
BJH average pore diameter (nm)	1.8	2.2
BJH single point total pore volume (c.c. g^{-1})	0.03	0.06

within a 0.5 mm capillary, was exposed to a wavelength of $\lambda = 0.774903$ Å.

2.3. Electrochemical characterization

The electrochemical characterization was performed using a CR2032 coin-type cell. The cathode consisted of 84 wt.% active material, 6 wt.% graphite powder (KS-4), 2 wt.% acetylene black and 8 wt.% poly(vinylidene fluoride) (PVDF) as a binder. The conductive carbon content of electrode is 8 wt.% (graphite powder and acetylene black). Electrodes were cast from the electrode slurry that contained the cathode active material, conductive carbon, binder and 1-methyl-2-pyrrolidinone (NMP) solvent. The electrode slurry was coated onto the aluminum foil current collectors and dried for 12 h in air, followed by 12 h in a vacuum oven at 383 K. The electrical resistance of the cast electrodes (pure LiFePO$_4$ and LiFePO$_4$/C samples) was measured by a four-point conductivity testing method. For charge and discharge test, samples with a diameter about 1.4 cm were punched from the cast electrode. The assembly of lithium half-cells in a CR2032 coin-type cell was performed in a dry room. The electrolyte was 1 M LiPF$_6$ dissolved in a mixture of ethylene carbonate (EC)/propylene carbonate (PC)/diethyl carbonate (DEC) (3:2:5 by volume). These Li/LiFePO$_4$ half-cells were galvanostatically cycled using the charger (Arbin) between 2 V and 4.2 V at room temperature. To get the high-power properties, these cells were tested with various discharge rates from 0.1 C to 12 C.

3. Results and discussion

3.1. Physical property and morphology

Typical synchrotron X-ray diffraction patterns of LiFePO$_4$ (pure) and LiFePO$_4$/C powders are displayed in Fig. 1, showing that these powders appear as single phases. X-ray Rietveld refinement indicated there was no extra electron density on the lithium site or iron
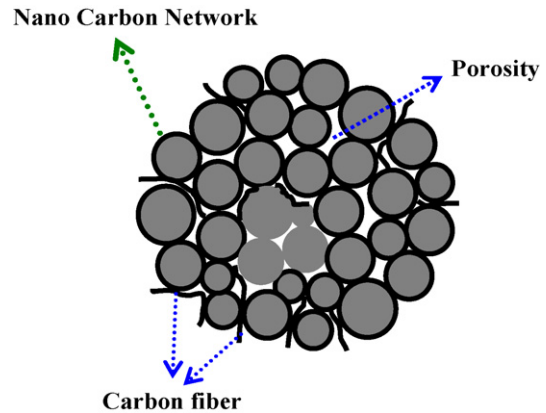

Fig. 4. The schematic representation of LiFePO$_4$/C powders with a continuous nano-carbon network.

disorder, and gave the following parameters for pure LiFePO$_4$: SG Pnma, $a = 5.978$ Å, $b = 10.608$ Å, $c = 4.82$ Å. The refinement parameters of LiFePO$_4$/C were close to the values of LiFePO$_4$ (pure). After carbon coating, the olivine structure of LiFePO$_4$/C was maintained with no evidence of impurities that may be caused by the reduction of iron during the carbon coating process. The tap density of pure LiFePO$_4$ (1.05 g cm^{-3}) was higher than that of LiFePO$_4$/C (0.85–0.9 g cm^{-3}) powder.

The electrical resistances of pure LiFePO$_4$ and LiFePO$_4$/C samples, measured by a four-point conductivity testing method, were 0.67 mΩ (LiFePO$_4$/C) and 43 KΩ (pure LiFePO$_4$). After a solid-state reaction, the carbon content of LiFePO$_4$/C powder was only 2.2 wt.%. However, the LiFePO$_4$/C composite cathode showed very low electrical resistance. Surface morphology shows that pure LiFePO$_4$ is denser than the LiFePO$_4$/C composite, as shown by the FE-SEM in Figs. 2 and 3, respectively. In Fig. 3(b), the LiFePO$_4$/C powder has a porous structure. As shown in Table 1, the LiFePO$_4$/C powders have larger surface areas (22 m^2/g) and bigger pore volumes (0.06 c.c. g^{-1}) than LiFePO$_4$ powder as a result of its porous structure. A particle-size analyzer measured the particle-size distribution of LiFePO$_4$/C powder between 1 μm and 20 μm. However, the surface area of the LiFePO$_4$/C sample was larger than that of other nano LiFePO$_4$ powder [8]. The shape of LiFePO$_4$/C powder is spherical and some pin-type carbon whiskers formed on the surface of LiFePO$_4$/C powder. The widths of the carbon whiskers are
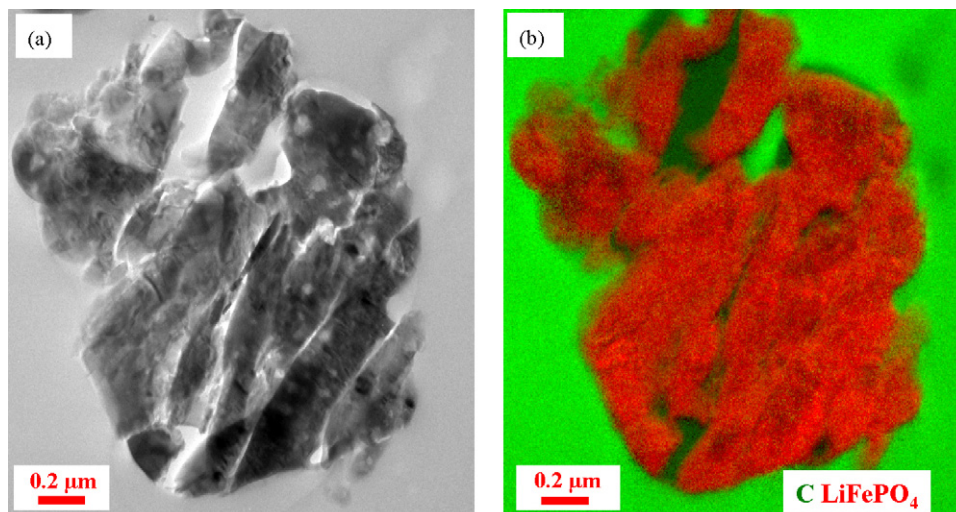

Fig. 5. (a)The transmission electron microscope bright field image and (b) EELS mapping of LiFePO$_4$ (pure) powders.
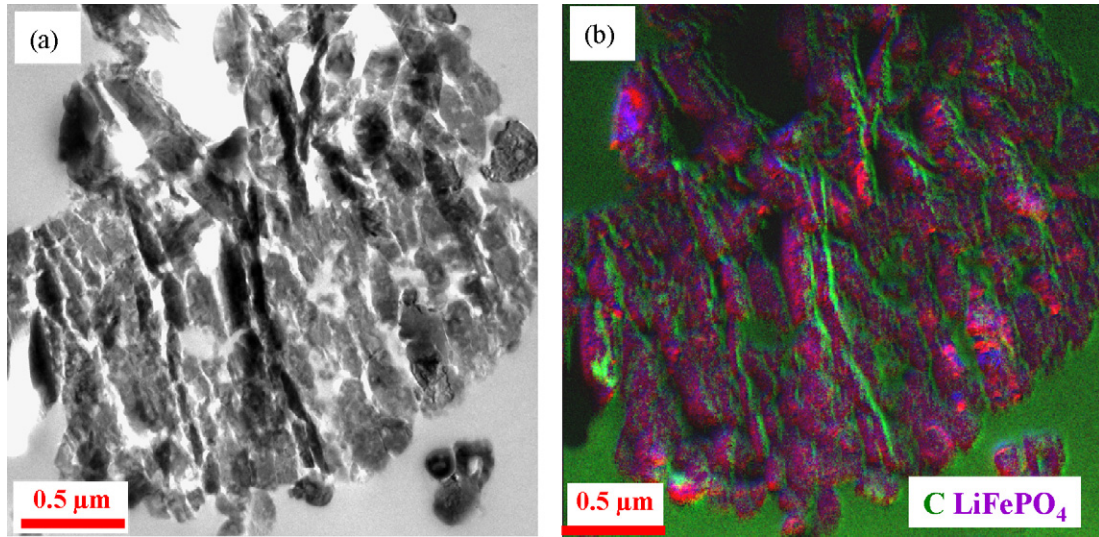
Fig. 6. (a)The transmission electron microscope bright field image and (b) EELS mapping of LiFePO$_4$/C powders.

about 0.5 μm and their lengths are between 1.5 μm to 3 μm. The LiFePO$_4$/C powders are composite cathode materials that have pin-type carbon whiskers and nano-carbon networks. This structure of composite cathode materials will improve electron transfer during high rate discharge. The schematic representation of LiFePO$_4$/C powder with pin-type carbon whiskers and a continuous nano-carbon network is shown in Fig. 4.

The transmission electron microscope bright field image and EELS mapping of pure LiFePO$_4$, show there was no significant carbon channel on the primary particle and only very few carbon signals (green parts on the primary particle in Fig. 5(b)). The carbon signal for the part outside of the primary particle is due to the sample holder. However, the transmission electron microscope bright field image and EELS mapping of LiFePO$_4$/C powder showed significant carbon signals (Fig. 6). The nano-carbon channels look like many streams on the plane that are shown in Fig. 6(b) and are continuous and dispersed in the core of LiFePO$_4$/C powder (inner part of the primary particle). These inner nano-carbon channels com-

bined with outer carbon surface coating will create a good carbon network. The width of nano-carbon channels are about 4–50 nm. In the lattice image of the LiFePO$_4$/C structure, the lattice fringe space is 2.8 Å and the thickness of the carbon layer is about 2–4 nm
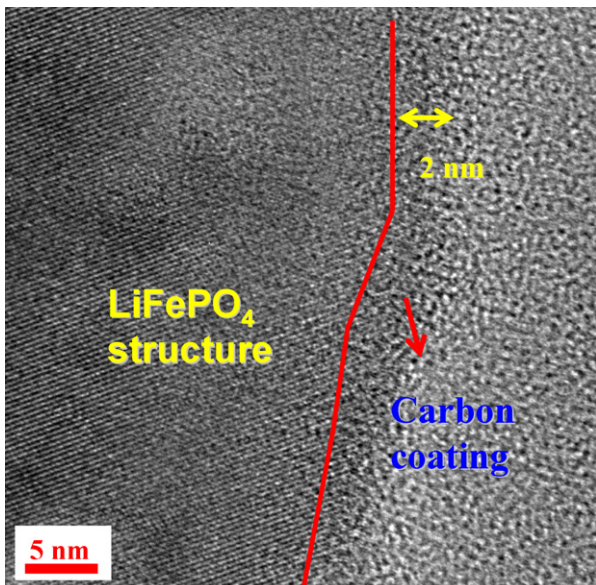

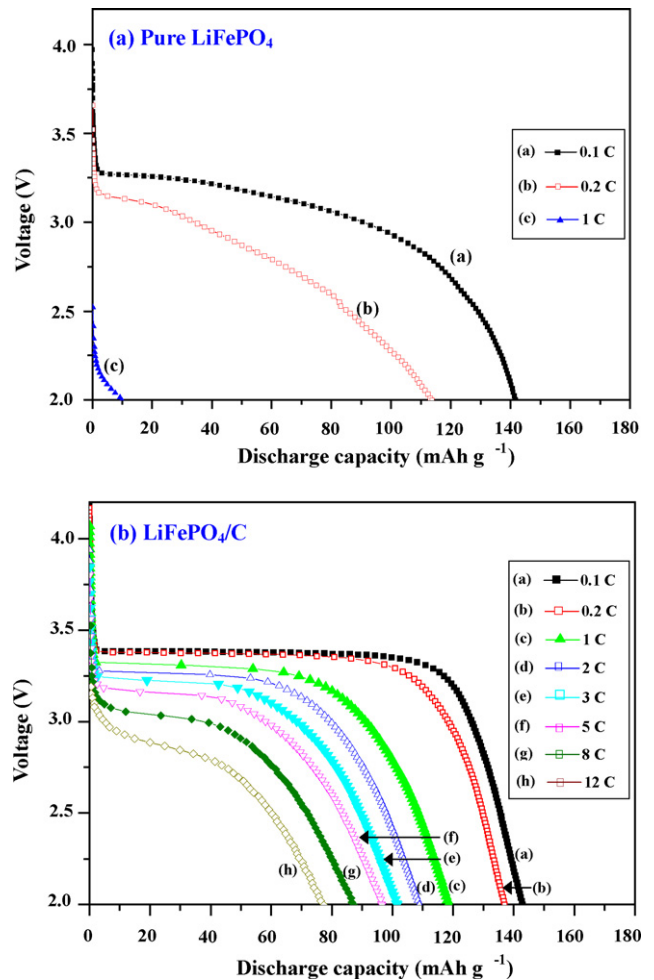**Fig. 7.** The lattice image of a LiFePO$_4$/C structure.

Fig. 8. The typical charge and discharge curves of (a) LiFePO$_4$ (pure) and (b) LiFePO$_4$/C cells.
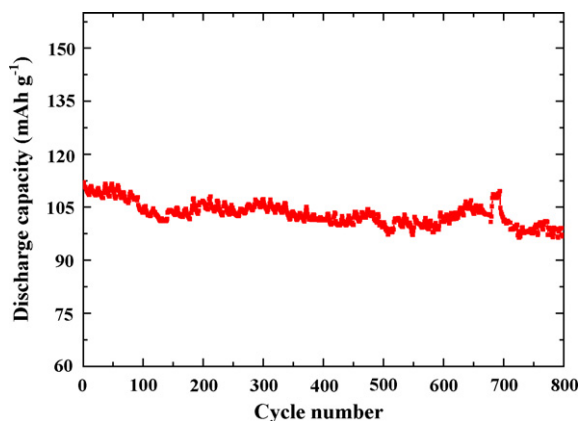
Fig. 9. The cycle life of a LiFePO$_4$/C cell at a 3 C rate (1 C charge and 3 C discharge).

(Fig. 7). The LiFePO$_4$/C composite cathode materials have a good carbon network and their porous structure improves the electrolyte immersion of LiFePO$_4$/C powders and shortens the diffusion distance for lithium ions.

3.2. Electrochemical performance

In order to find the working voltage and high-power properties of LiFePO$_4$/C composite powders, the LiFePO$_4$/C cells were charged and discharged at different rates. Fig. 8 shows the typical discharge curves of LiFePO$_4$ (pure) and LiFePO$_4$/C cells that used the lithium metal as a counter electrode. The specific capacity of the LiFePO$_4$/C cell (140 mAh g^{-1}) was higher than that of LiFePO$_4$ cell (115 mAh g^{-1}) at a 0.2 C rate. Under a 1C-rate discharge test, the specific capacity of undoped LiFePO$_4$ cathode material was very low (10 mAh g^{-1}) because of its much higher electrical resistance (43 KΩ). It is obvious that the LiFePO$_4$/C composite cathode materials were superior in specific capacity, rate capability and cycle life to the LiFePO$_4$ (pure) cathode material. At a high rate discharge, the LiFePO$_4$/C cell showed good rate capability. The discharge capacity ratio for $Q_{12\,C}/Q_{0.2\,C}$ was more than 60%. The discharge curves of a LiFePO$_4$/C cell at different current rates are plotted in Fig. 8(b), which indicates that the capacity was strongly affected by the discharge current, especially in the high current range. The cycle life of the LiFePO$_4$/C cell during high-rate discharge (3 C) was excellent even after more than 700 cycles with little capacity fading (Fig. 9). In this case, the cell was galvanostatically cycled with a 1 C rate charge and 3 C rate discharge from 2 V to 4.2 V at room temperature. The LiFePO$_4$/C cell exhibited stable capacity with increasing

cycle numbers. These results clearly demonstrate that the coating olivine particles with a nano-carbon layer (2–4 nm) significantly improved electronic conductivity of LiFePO$_4$ cathode materials. From Figs. 3 and 6, the LiFePO$_4$/C material has shown the continuous and dispersive nano-carbon network and porous structure. The nano-carbon networks have increased high conductivity of the cathode and good electron transfer in the structure of LiFePO$_4$/C composite cathode materials. From Fig. 3 and Table 1, the LiFePO$_4$/C composite cathode material displays a porous structure with high surface area and pore volume which will improve the electrolyte immersion of LiFePO$_4$/C powders and shorten the diffusion distance of lithium ions.

4. Conclusions

The continuous and dispersive nano-carbon network greatly improved the cathode conductivity and electron transfer of lithium ions in the LiFePO$_4$ structure, which led to good electrochemical performance. The LiFePO$_4$/C particles that have high surface areas and pore volumes show continuous and dispersive nano-carbon network. This kind of conductive carbon network has demonstrated that the LiFePO$_4$/C composite cathode material was capable of high-rate discharge and long cycle life.

Acknowledgment

References

[1] A.K. Padhi, K.S. Nanjundaswamy, J.B. Goodenough, J. Electrochem. Soc. 144 (1997) 1189.
[2] A. Yamada, S.C. Chung, K. Hinokuma, J. Electrochem. Soc. 148 (2001) A224.
[3] A. Yamada, S.C. Chung, J. Electrochem. Soc. 148 (2001) A96.
[4] S. Yang, Y. Song, P.Y. Zavalij, M.S. Whittingham, J. Electrochem. Commun. 4 (2002) 239.
[5] J.D. Wilcox, M.M. Doeff, M. Marcinek, R. Kostecki, J. Electrochem. Soc. 154 (2007) A389.
[6] I. Belharouak, C. Johnson, K. Amine, J. Electrochem. Commun. 7 (2005) 983.
[7] F. Croce, A.D. Epifanio, J. Hassoun, A. Deptula, T. Olezac, B. Scrosati, Electrochem. Solis-State Lett. 5 (2002) A47.
[8] M. Takahashi, S. Tobishima, K. Takei, Y. Sakurai, J. Power. Sources 97–98 (2001) 508.
[9] S.Y. Chung, J.T. Bloking, Y.-M. Chiang, Nat. Mater. 1 (2002) 123.
[10] Z. Chen, J.R. Dahn, J. Electrochem. Soc. 149 (2002) A1184.
[11] C. Wurm, M. Moorcette, S.Gwizdala, and C. Masquelier, Word Pat. WO 02/099913 A1 (2002).
[12] N. Ravet, Y. Chouinard, J.F. Magnan, S. Besner, M. Gauthier, M. Armand, J. Power. Sources 97–99 (2001) 503.
[13] H. Huang, S.C. Yin, L.F. Nazar, Electrochem. Solis-State Lett. 4 (2001) A170.